Werk

Jahr: 1978
Kollektion: fid.geo
Signatur: 8 Z NAT 2148:45
Digitalisiert: Niedersächsische Staats- und Universitätsbibliothek Göttingen
Werk Id: PPN1015067948_0045
PURL: http://resolver.sub.uni-goettingen.de/purl?PPN1015067948_0045

LOG Id: LOG_0014
LOG Titel: Observations of the initial develpopment of an auroral and magnetic substorm at magnetic midnight
LOG Typ: article

Übergeordnetes Werk

Werk Id: PPN1015067948
PURL: http://resolver.sub.uni-goettingen.de/purl?PPN1015067948
OPAC: http://opac.sub.uni-goettingen.de/DB=1/PPN?PPN=1015067948

Contact

Niedersächsische Staats- und Universitätsbibliothek Göttingen
Georg-August-Universität Göttingen
Platz der Göttinger Sieben 1
37073 Göttingen
Germany
Email: gdz@sub.uni-goettingen.de

J. Geophys. 45, 41–65, 1978

Journal of Geophysics

Observations of the Initial Development of an Auroral and Magnetic Substorm at Magnetic Midnight

J. Untiedt[1], R. Pellinen[2], F. Küppers[1], H.J. Opgenoorth[1], W.D. Pelster[1], W. Baumjohann[1], H. Ranta[3], J. Kangas[4], P. Czechowsky[5], and W.J. Heikkila[6]

[1] Institut für Geophysik der Universität Münster, Gievenbecker Weg 61, D-4400 Münster, Federal Republic of Germany

[2] Division of Geomagnetism, Finnish Meteorological Institute, Vuorikatu 24, Bos 503, SF-00100 Helsinki 10, Finland

[3] Geophysical Observatory, SF-99600 Sodankylä, Finland

[4] Dept. of Physics, University of Oulu, Linnanmaa, SF-90100 Oulu 10, Finland

[5] Max-Planck-Institut für Aeronomie, Postfach 20, D-3411 Katlenburg-Lindau 3, Federal Republic of Germany

[6] Center for Space Sciences, University of Texas at Dallas, Richardson, Texas 75080, USA

Abstract. On April 6, 1975 a rather well isolated magnetic substorm began with a sharp onset at 2122 UT one hour after a clear southward turning of the interplanetary magnetic field. We report on results of observations obtained with meridian chains of magnetometers, all sky cameras, riometers, and short period pulsation magnetometers, plus additional stations and equipment, one hour before and a few minutes around the onset of a substorm at magnetic midnight within the Scandinavian area.

The time interval before onset was mainly characterized by an auroral arc which drifted southward in parallel with a westward electrojet and with a bay-like weak absorption region. The arc being located above the northern half of the electrojet showed intermittent local distortions, including a mature spiral, which in each case was accompanied by local pi B type magnetic pulsations. The spiral enclosed a region of upward directed field-aligned current as inferred from local distortions of the magnetic field at ground. Possibly the electrojet was due to a large-scale westward electric field, with the intensity of the corresponding field-aligned currents amounting to values of the order of 1 Akm^{-2} at the time when auroral distortions first appeared.

At substorm onset, the westerly part of the midnight auroral breakup region seems to have been observed by our all-sky cameras. This region was also characterized by strong cosmic noise absorption; it was surrounded by an anticlockwise (if viewed from above) differential equivalent current vector circulation, which indicates that the breakup occurred below a region of intense upward field-aligned currents switched on during substorm onset. Such a conclusion seems to be supported by our simultaneous radio wave backscatter amplitude and Doppler shift observations.

Key words: Auroral substorm – Magnetic substorm – Growth phase – Auroral electrojet – Auroral loops.

0340-062X/78/0045/0041/$05.00

1. Introduction

Numerous papers have been written on the magnetospheric substorm based on results of satellite, rocket, balloon, and ground based observations. The general pattern of the substorm both on the global and on the magnetospheric scale seems to be rather well known, and has been described in several monographs and review articles (e.g., Akasofu, 1968, 1977; Rostoker, 1972; Russell and McPherron, 1973). However, because of limited observation facilities there are many details of the picture for which an accurate description both in space and time is still impossible. Also, the physical relationship between the different phenomena occurring at the same time is rather unclear, in many cases. Near the earth this is especially true for the very limited area of the auroral oval close to magnetic midnight where the breakup phase of the auroral substorm usually occurs. Our present paper reports on ground based observations of different types made under this area when it was situated over Northern Scandinavia on April 6, 1975, one hour before and during the early expansion phase of a rather isolated substorm.

The instruments from which data have been used in our study include meridian chains of all-sky cameras, of magnetometers, and of riometers. Among others, additional data were available from a radio-wave backscatter facility measuring both signal intensity and Doppler shift, and from several pulsation magnetometers.

Originally, the event was selected because of its remarkably large steplike magnetic D disturbance occurring at the time and near the location of the auroral breakup. Later, it was found that the one hour interval before this magnetic onset, possibly constituting a substorm growth phase (McPherron, 1970), also exhibited interesting relationships between the local magnetic and auroral phenomena.

2. Instruments

Within this section we give a short description of the main instruments from which data have been used in the present study. The location and other details of each instrument may be taken from Fig. 1 or from Table 1.

The five all-sky cameras set up by the Finnish Meteorological Institute approximately in a north-south chain are of a new design (Hyppönen et al., 1974), with digital time display accurate to the nearest second. The 16 mm colour film is processed to ASA rating 1000, permitting an exposure time of 2 s. Radioactive sources were used to activate calibration surfaces visible on each photograph, for calibrations within both the red and green parts of the spectrum. During the time interval considered in this study the stations were run at the rate of one frame per minute, with the one exception of Ivalo. There, due to a fortunate malfunction, the camera operated at eight frames per minute just around the time of the auroral breakup.

In order to compare the locations of aurorae relative to other observed phenomena, structures like arcs, spirals etc. have been digitized, rectified, and

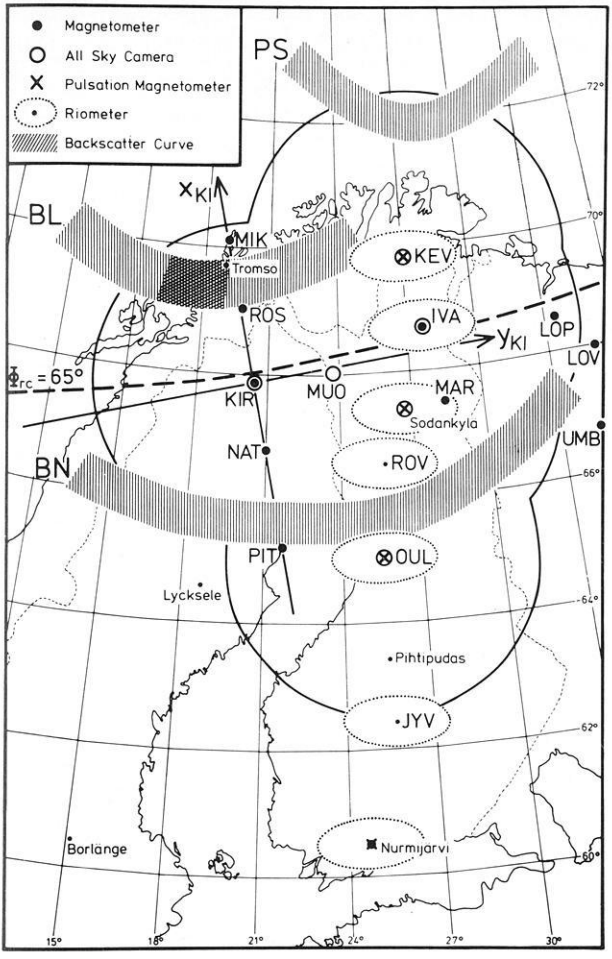

Fig. 1. Map of stations situated within Scandinavian area. Observational coverage through all-sky cameras is indicated by a solid curve (as defined by 70° elevation angle and 110 km height); corresponding coverage of each riometer is represented by a dotted curve. Backscatter curves: PS: transmitter at Pihtipudas, receiver at Sodankylä; BL and BN: transmitter at Borlänge, receiver at Lycksele and Nurmijärvi, respectively. Crosshatched part of curve BL corresponds to narrow beam receiver. The x_{KI}, y_{KI} coordinate system which is being used widely within this study, is also shown. The broken line denoted by $\phi_{rc}=65°$ represents a curve of constant revised corrected geomagnetic latitude. For more explanation see text

mapped assuming a height of 100 km (Boyd et al., 1971). If possible, lower borders of aurorae were used during the digitization process. In most cases, the same auroral structure was digitized from photographs of several cameras and the results were compared after mapping. Generally the mapped structures coincided within about 20 km, with the exception of weak aurorae or structures recorded at low elevation angles.

For the present study, magnetograms were available from the first five stations of the University of Münster magnetometer array that has been installed

Table 1. Permanent or temporary stations from which data have been used, mainly, in the present study

Station	Symbol	Geograph. Coord.		RCGL[a]	Type of instrument[b] and running institution[c] (in brackets)		
Ny Alesund	NYA	78.9°N	11.9°E	75.9°	M(AOT)		
Bear Island	B4	74.5	19.0	71.3	M(AOT)		
Mikkelvik	MIK	70.1	19.0	67.1	M(UM)		
Rostadalen	ROS	69.0	19.7	66.0	M(UM)		
Kiruna	KIR	67.8	20.4	64.8	M(UM)	ASC(KGI)	
Nattavara	NAT	66.8	21.0	63.7	M(UM)		
Pitea	PIT	65.2	21.6	62.2	M(UM)		
Kevo	KEV	69.8	27.0	66.2		ASC(FMI)	R, P
Ivalvo	IVA	68.6	27.5	65.0	M(TUB)	ASC(FMI)	R
Muonio	MUO	68.0	23.6	64.8		ASC(FMI)	
Sodankylä	SO	67.4	26.6	63.9		ASC(FMI)	R, P
Martii	MAR	67.5	28.3	63.9	M(TUB)		
Rovaniemi	ROV	66.6	25.8	63.2			R
Oulu	OUL	65.1	25.5	61.8		ASC(FMI)	R, P
Jyväskylä	JYV	62.4	25.7	59.0			R
Nurmijärvi	NU	60.5	24.6	57.0	M(FMI)		R, P
Loparskaya	LOP	68.6	33.3	64.7	M(PGIA)		
Lovozero	LOV	68.0	35.0	64.1	M(PGIA)		
Umba	UMB	66.7	34.5	62.9	M(PGIA)		

[a] Revised Corrected Geomagnetic Latitude (Gustafsson, 1970)
[b] M: magnetometer; ASC all-sky camera; R: riometer; P: pulsation magnetometer
[c] If not explained unambiguously within text;
FMI: Finnish Meterorological Institute; UM: University at Münster; TUB: Technical University at Braunschweig; KGI: Kiruna Geophysical Institute; PGIA: Polar Geophysical Institute at Apatity; AOT: Auroral Observatory at Tromsö

stepwise in 1974–1976 for groundbased observations during the International Magnetospheric Study (IMS, 1976–1979) in Scandinavia (Küppers et al., 1979). The instruments are improved versions of the Gough-Reitzel magnetometer (Gough and Reitzel, 1967). They yield analog records with 1–2 nT or 2% of amplitude accuracy, and better than 10 s time resolution and accuracy. The five stations are located on a straight profile oriented perpendicularly to the line of constant revised corrected geomagnetic latitude (Gustafsson, 1970) that is intersected at Kiruna.

In addition to these five stations, magnetograms from several nearby magnetic observatories or temporarily installed magnetic stations have been used (cf. Table 1). The latter are two stations equipped with flux-gate magnetometers and digital recording that are being operated by H. Maurer, Technical University of Braunschweig, and three stations with analog recording run by the Polar Geophysical Institute at Apatity on the Kola peninsula (USSR). The time accuracy of these additional magnetic data was about 1 min due to a clock malfunction or reading errors within copies, respectively.

A north-south chain of seven 27.6 MHz riometers was operated by the Geophysical Observatory at Sodankylä on a routine basis. Four additional

riometers of frequencies 20 MHz, 40 MHz, and 50 MHz were operated at Sodankylä. The data were recorded with a chart speed of 60 mm/h, allowing one minute time resolution.

Observation of radio aurora is another method by which disturbances in the polar E-region may be studied, although the mechanism by which the scattering irregularities are generated is not yet understood completely (Egeland, 1976). During the substorm under consideration, signals recorded by three bistatic CW – backscatter equipments supplemented the other observations. One transmitter was operated at Borlänge (Fig. 1) at a frequency of 145 MHz. Its backscattered signals were received at Lycksele and Nurmijärvi. Another transmitter (97 MHz) was located at Pihtipudas, with a receiving station being operated at Sodankylä. The corresponding three backscatter regions within the ionospheric E-region are quite confined in latitude due to aspect angle dependence. They are rather evenly distributed over Northern Scandinavia (Fig. 1). It was important for our study that the station at Lycksele operated by the Max-Planck-Institut für Aeronomie, Lindau/Harz, was equipped with two receiving antennas of different beam widths. The half power beam width of receiver A mounted to 37 degrees, whereas that of receiver B was only 10 degrees. For receiver B this resulted in a backscatter volume also correspondingly confined in longitude, and located a little southwest of Tromsö (Fig. 1). Furthermore, both receivers were able to record the mean Doppler shift of the backscattered signal.

Magnetic pulsation recordings were available from four permanent stations in Finland. They are run by the University of Oulu and the Geophysical Observatories at Sodankylä and Nurmijärvi, and are equipped with induction coil magnetometers that are most sensitive between 0.1 Hz and 1 Hz. The time resolution is better than half a minute.

3. Observations

General Situation

The substorm under consideration occurred on April 6, 1975 between 20 and 23 UT when northern Scandinavia was located under the midnight sector of the auroral oval. Near the center of this region, e.g., at Ivalo (IVA, Fig. 1) corrected geomagnetic midnight was at 2120 UT (Whalen, 1970). The substorm seems to have been isolated rather well. As demonstrated by Figure 2 the well-known magnetic observatories along the auroral zone, as well as midnight-sector low latitude stations, exhibited only small shifts or fluctuations within the horizontal components between 18 and 20 UT. The shifts may partly be due to the late recovery phase of another though weaker substorm period that started between 14 and 15 UT. The magnetic quietness between the two substorms is also indicated by the absence of any Pi 2 activity between 16 and 21 UT at middle European observatories which were located within the evening sector during this time (H. Voelker, pers. comm.).

Simultaneously, the interplanetary magnetic field showed the following characteristics according to observations by the satellite IMP-J which was located

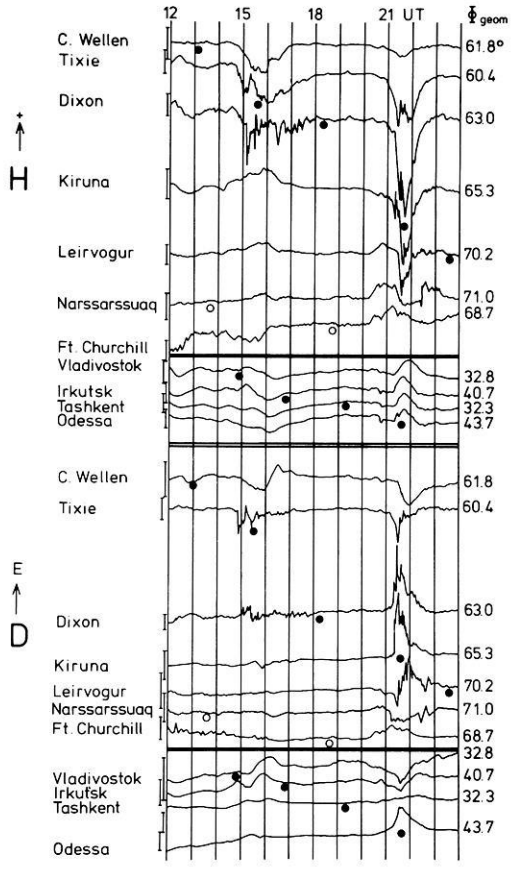

Fig. 2. Variations of horizontal components along the northern hemisphere auroral zone and at four stations from the southern part of the USSR on April 6, 1975. Scale bars correspond to 50 nT for the four low latitude stations, and to 200 nT otherwise. Magnetic midnight and midday (after Whalen, 1970) are denoted by full and open circles, respectively

at the point (-0.6, -21.5, 18.8) as measured in geocentric solar magnetospheric coordinates (Russell, 1971): Between 1800 and 2016 UT the field was northward with the exception of two short southward excursions at 1904 and 1920 UT, with a duration of about 2 min each. There are data gaps around 2000 and 2010 UT each lasting for about 5 min. At 2016 UT a sharp change to the southward direction occurred. This direction persisted until 2133 UT when the field gradually became northward and essentially stayed in this way for the next 2 h (J. Vette, pers. comm.).

The general character of the substorm as observed over the Scandinavian region is shown by the magnetograms in Figure 3. Here, the horizontal field is represented by its components A and B. They are defined as being parallel to the x_{KI} axis and the y_{KI} axis, respectively, that are shown in Fig. 1. This cartesian system has been introduced by Küppers et al. (1979). It is applicable only within a limited region, because projection onto a tangential plane is the basic assumption. The adopted plane is tangent to the globe at Kiruna. At this point the x_{KI} or A direction is chosen as to be orthogonal to the line of constant revised corrected geomagnetic latitude (Fig. 1). The A variations

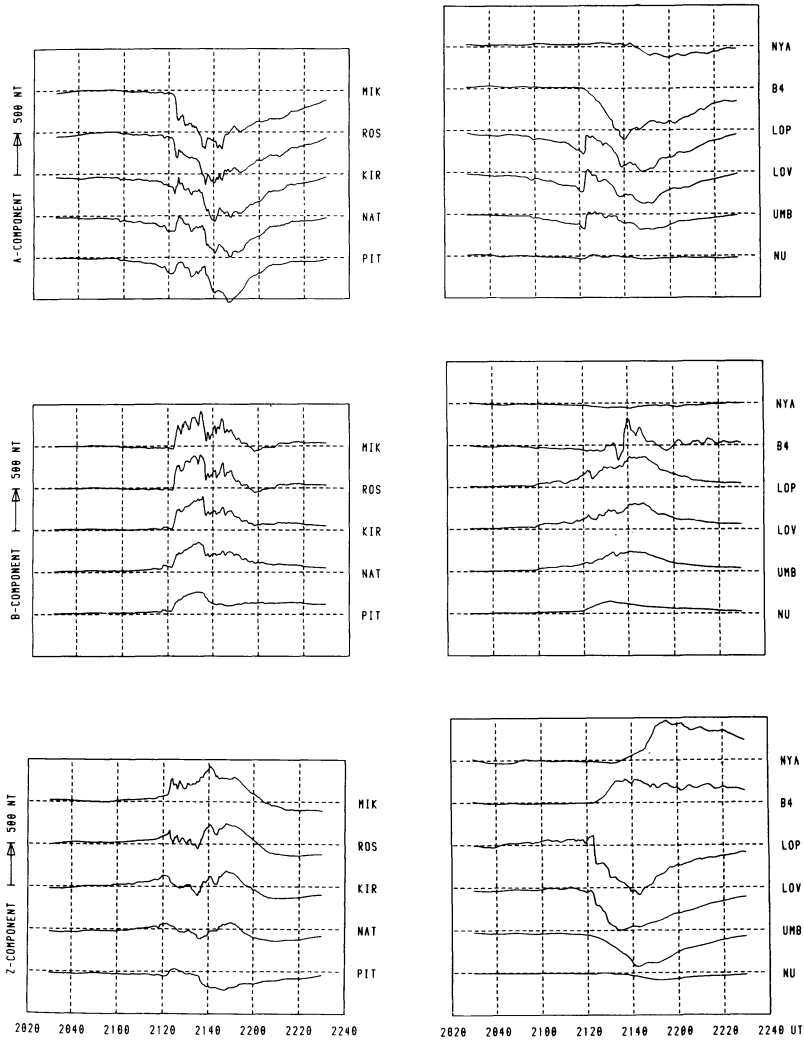

Fig. 3. Magnetic variations on April 6, 1975 at selected stations within and around the Scandinavian area. Stations B4 and NYA (see Table 1) are not shown within Figure 1. A and B denote horizontal components parallel to x_{KI} and y_{KI} axis (shown in Fig. 1), respectively. Z positive downwards. Horizontal lines corresponding to undisturbed levels

generally are rather similar to the usual *H* variations, and the same similarity exists between B and D.

In Fig. 3, magnetograms to the left are from the University of Münster chain and those to the right from islands north of Scandinavia, from the Kola peninsula to the east, and from southern Finland (cf. Fig. 1 and Table 1). Before 2040 UT the traces are close to the quiet time level which for each station and component is represented by the horizontal broken line.

As judged from the A and Z traces in Fig. 3, the substorm is governed by a broad westward electrojet. It flows above and northward of our region

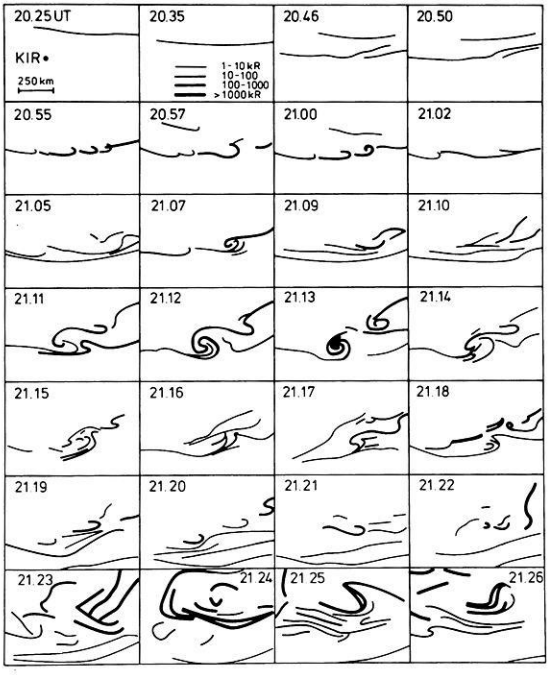

Fig. 4. Montage of maps showing position of linear auroral forms above northern Scandinavia at different moments on April 6, 1975. Results of analysis of digitized and rectified data from several all-sky cameras (see text). x_{KI} axis is oriented upwards, y_{KI} axis to the right (cf. Fig. 1). Position of Kiruna ($x_{KI}=y_{KI}=O$) is shown on the first map, intensity scale on second map

and reaches its maximum strength corresponding to a magnetic 500 nT disturbance at ground around 2145 UT, i.e., around local magnetic midnight. The same electrojet is evident in the H traces from Narssarssuaq (Greenland) and Leirvogur (Iceland) to the west and from the stations along the northern coast of the Soviet Union, to the east (cf. Fig. 2). The magnetic observatories at lower latitudes within the midnight sector see a typical bay disturbance most pronounced in the D component which changes sign at around 02 MLT (Fig. 2). The latter fact indicates that the central meridian of a Birkeland type ionospheric-magnetopheric current system (e.g., according to Meng and Akasofu, 1969) capable to explain these main substorm characteristics probably is located 2 h eastward from our region.

The onset of the main substorm phase occurred at about 2122 UT as indicated by the high and low latitude magnetograms (Fig. 2 and 3) which show strong inflections of all components at this time, and by Pi 2 activity as observed in middle and northern Europe. We concentrate our present study on the preceding hour and on the few minutes around this onset.

Figure 4 gives a synopsis of the auroral activity over northern Scandinavia throughout this time interval. Fair weather conditions permitted good observations from twilight at around 1940 UT on, when a faint arc was located about 70 km north of our northernmost all sky camera station Kevo. Later this arc, and also intermittently appearing additional arcs, underwent different intensifications and foldings until between 2122 and 2123 UT the breakup occurred. Throughout most of the time auroral arcs travelled southward and structures to the east.

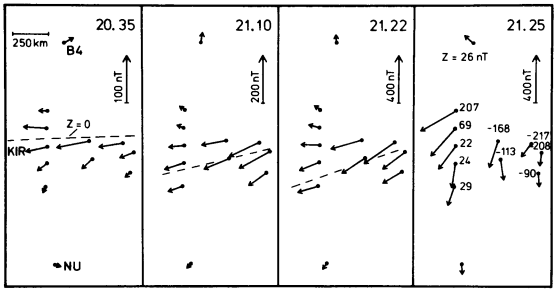

Fig. 5. Equivalent current vectors at selected moments (UT) within and around Scandinavia. Orientation of axes as in Figure 4. Position of three magnetic stations is indicated on first map. Numbers on fourth map give Z values (nT). Broken lines indicate curve where Z=0 (estimated from Z values observed at stations). Note different magnetic scales

A corresponding synopsis of the magnetic field development within about the same region is given by Figure 5 which shows equivalent current vectors, i.e., horizontal magnetic disturbance vectors rotated 90 degrees clockwise if viewed from above. The equivalent current flow changes slowly from a westward direction (as defined within the x_{KI}, y_{KI} system) towards a more southwestern flow until 2122 UT when a sudden deflection occurs towards a southern direction at the time of the main onset (cf. flow pattern at 2125 UT). As indicated by the different scale marks within Figure 5, the intensity of the currents increases by a factor of 4 between 2035 and 2122 UT but remains of the same order of magnitude over the magnetic onset.

Pre-Onset Period (2025-2122 UT)

During the one hour preceding the onset the magnetograms from the high latitude stations around the globe (some of which are illustrated in Fig. 2) indicate increasing eastward equivalent current flow (see H components from Narssarssuaq and Leirvogur) if westward from our region, i.e., if the stations are located in the afternoon and evening sector, and vice versa. The evening sector eastward flow extends into the polar cap according to the magnetogram (not shown) from Upernavik (western Greenland). At midlatitudes in the midnight sector (e.g., Odessa in Fig. 2) increasing D components indicate increasing southward flow during the same time interval.

These magnetic observations point to a high-latitude equivalent current system of the twin-vortex mode including two electrojets, as described for example by Troshichev et al. (1974). It may be assumed that this system is mainly due to magnetospheric convection starting to increase at the time of southward turning of the interplanetary magnetic field, as mentioned above. The southward and eastward auroral motions observed over Scandinavia fit into this picture (Vorobjev et al., 1976).

The average southward motion of the southernmost arc between 2025 and 2120 UT (Fig. 4) amounts to 120 ms^{-1}. Because we are close to magnetic midnight where the auroral oval is east-west aligned this motion may directly indicate an expansion of the oval. On the other hand, southward velocities of this magnitude are regularly observed for individual auroral forms independent of the oval behaviour at this time of the day (Snyder and Akasofu, 1972; Vorobjev

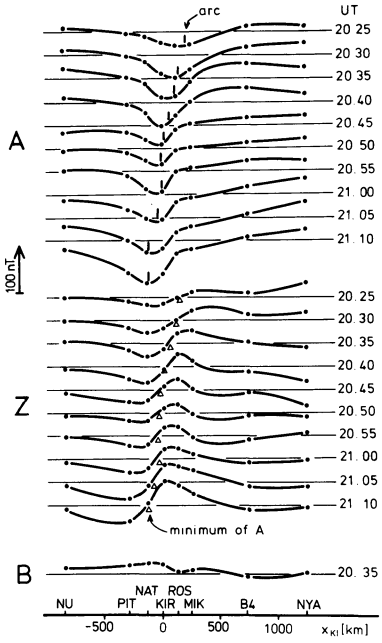

Fig. 6. Latitude profiles of different magnetic components at selected equidistant moments well before substorm onset (auroral breakup). Horizontal lines correspond to undisturbed levels. The position of the southernmost auroral arc is indicated at the A profiles, position of A minimum likewise indicated at Z profiles. Only one B latitude profile shown, as an example

et al., 1975). It should be mentioned that Lassen et al. (1977) who recently performed a case study partly similar to the present one, have found a southward drift of the preexpansive phase arc after the southward turning of the interplanetary magnetic field in the evening sector only, but not around midnight.

The westward or southwestward equivalent current flow observed over Scandinavia before 2122 UT mainly consists of a rather narrow electrojet, according to the latitude profiles of A and Z shown by Figure 6. The current is centered a little south of the southernmost (and for most of the time solely observed) auroral arc (cf. vertical bars within A latitude profiles), and remarkably follows its southward motion. Some spatial relationship between auroral arcs as observed by the ISIS 2 satellite and eastward and westward electrojets (generally of a larger width than in our case) has already been studied by Wallis et al. (1976), but here we are able to show that electrojet and arc travel with about the same southward speed. As will be discussed below this holds even for the case when the speed undergoes temporal variations.

According to the B latitude profiles, of which only one typical example is shown in Figure 6, the electrojet is not of a two-dimensional nature. This is also evident from Figure 5. For the time interval under consideration, the magnetic observations may be modelled by a Birkeland type current loop consisting of a homogeneous ionospheric electrojet of finite length with corresponding up- and down-flowing field aligned currents at its ends, according to the method described and applied extensively by Kisabeth (1972; see also Kisabeth and Rostoker, 1977). If we compare our latitude profiles with those given by Kisabeth (1972) for different model Birkeland current loops we may draw the conclusion that we are under the western half of the electrojet and that as a first approxima-

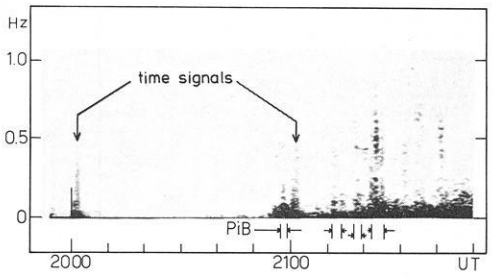

Fig. 7. Spectrogram of short period magnetic pulsation activity at Sodankylä on April 6, 1975. Pi B events are denoted

tion end effects and the effects of the field-aligned currents may be neglected within A and Z components. That we are still far enough from the ends of the electrojet follows from the fact that the total variation within the B profiles is considerably smaller than the total variation within the corresponding Z profiles.

The development of auroral activity will now be described a little more in detail (cf. Fig. 4). In addition to the main arc which had intensified and narrowed showing slight distortion for the first time, at 2046 UT a second faint arc became visible about 120 km to the north but disappeared after a few minutes. At about 2054 UT the main arc intensified and simultaneously developed into a chain of hook-like folds that travelled towards the east with a velocity of 1–2 km s^{-1}. At the same time the first Pi B event (impulsive broadband Pi burst, see Heacock, 1967) of this night was detected by the short-period pulsation magnetometers at Sodankylä and also, with smaller amplitudes, at Oulu and Nurmijärvi (cf. spectrogram from Sodankylä as shown in Fig. 7). Around the time of this auroral disturbance which persisted only for 8 min, the magnetic A latitude profiles (Fig. 6) became more asymmetrical by exhibiting stronger gradients at the northern border of the electrojet region than at the southern one. Corresponding deformations (a more pronounced northern maximum) are to be seen in the Z profiles.

At 2107 UT a short-lived spiral-like structure appeared over the eastern part of our region followed by wavy or hook-like weak disturbances. By 2110 UT all auroral activity had reduced to several faint arcs. Immediately thereafter, an intense well-defined stationary auroral spiral (Davis and Hallinan, 1976) developed. It showed an anticlockwise winding-up (if viewed from above) of former rectilinear structures. This sense of rotation is always observed for spirals (Davis and Hallinan, 1976) and is due to a magnetic shear caused by a concentration of upward field-aligned currents according to the theory proposed by Hallinan (1976).

During the few minutes of spiral formation, which culminated at 2113 UT, some slight distortion of the equivalent current distributions occurred. These distributions were otherwise similar to the example shown in Fig. 5 for 2110 UT. In order to see if this distortion might be ascribed directly to the auroral spiral the difference of the equivalent current vectors between 2110 and 2113 UT has been mapped in Figure 8. This method is analogous to the use of differential latitude profiles of magnetic components introduced by Kisabeth (1972). Figure 8 clearly shows that over the time interval of spiral growth an equivalent

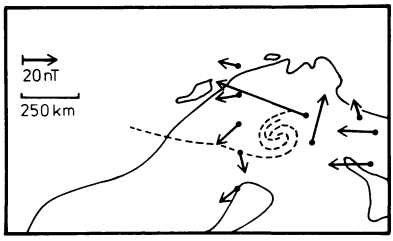

Fig. 8. Position of auroral spiral (dotted) at 2113 UT, and differential equivalent current vectors calculated for the time difference 2110 and 2113 UT (i.e., currents being added over this interval)

current pattern is being added to the formerly existing one that exhibits an anticlockwise current circulation around the spiral center. Such an equivalent current loop will be generated (Fukushima, 1971) if a vertical upward directed field-aligned line current is escaping from a laterally homogeneous or rotationally symmetric ionosphere. The field-aligned current would be fed by radially inward directed Pedersen currents (cf. Fig. 15 below) that compensate its magnetic field below the ionosphere. Therefore, only the magnetic field of the circular Hall currents will be detectable at the ground.

Accordingly, our observations seem to indicate that during spiral formation there is a local addition or concentration of upward field-aligned current, as predicted by the theory of Hallinan (1976). Similar conclusions have been drawn by Wescott et al. (1975) from the results of a barium plasma injection experiment.

Like the auroral activity at 2055 UT the beginning of spiral development was accompanied by a Pi burst at 2111 UT (Fig. 7). Another Pi B appeared at 2116 UT when the last auroral intensification before breakup began. Again, hook-like folds travelled rapidly towards east. Simultaneously, the first Pi 2 event was recorded at middle European magnetic observatories (e.g., Wingst and Göttingen).

At the same time an onset of weak backscattering of radio waves from auroral structures was noticed at Sodankylä (corresponding to the backscatter region PS in Fig. 1), but probably not at Lycksele (region BL) and undoubtedly not at Nurmijärvi (region BN). Afterwards, at 2119 UT a nearly total fading of backscatter intensity occurred, as well as in auroral activity. According to all-sky photographs, the northern sky became especially dark, in agreement with the pre-breakup observations reported by Snyder and Aksofu (1972). Auroral fading seems to be a phenomenon regularly occurring before breakup as has been reported and discussed by Pellinen and Heikkila (1978).

During the time before breakup and main substorm onset, the riometers from the Finnish chain had already indicated some weak absorption (Fig. 9) which started around 2030 UT above Ivalo (and possibly above Kevo where heavy fluctuations all the time impeded interpretation of the data) and later and more gradually above Sodankylä, Rovaniemi and Oulu. A southward shift or expansion of the absorption region can be inferred from Figure 9 yielding a speed of 100–200 ms^{-1}. According to Hargreaves et al. (1975) who like others (Pytte et al., 1976) regularly observed this phenomenon, the pre-onset bay-like equatorward moving absorption activity is indicative of inward convection of energetic plasma in the magnetosphere and should be regarded as evidence

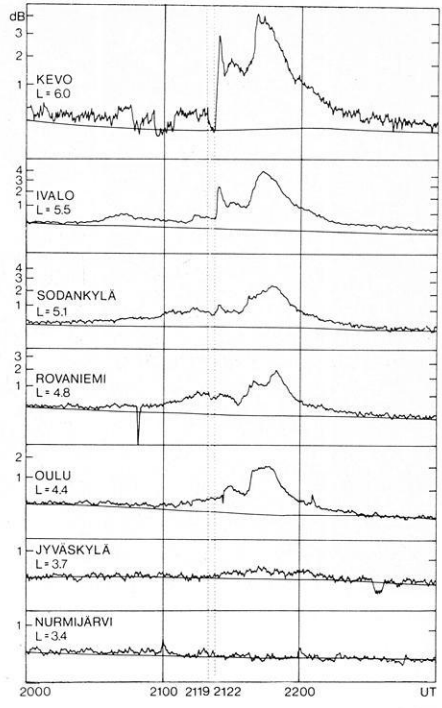

Fig. 9. Cosmic noise absorption as recorded by the Finnish riometer meridian chain on April 6, 1975. Undisturbed levels are indicated

for a substorm growth phase. Note that in our case the absorption region drift is of the same direction and magnitude as the average drift observed simultaneously for the southernmost auroral arc and the westward electrojet within the same region (cf. Fig. 6, or Fig. 12a and b, below).

Around 2113 UT the absorption was slightly increased above Ivalo and probably above Sodankylä, possibly in relation to the spiral formation which has been discussed above. Between 2119 and 2122 UT (i.e., just before substorm onset and auroral breakup), the absorption decreased clearly above Sodankylä and Rovaniemi and most strongly above Kevo. This phenomenon is well known especially from balloon-borne X-ray measurements (Pytte and Trefall, 1972; Pytte et al., 1976).

Auroral Breakup and Magnetic Onset

After the last auroral fading mentioned, an intensive hooklike structure developed rather far to the west (a little south of Kiruna) at 2119:30 UT (cf. Fig. 4). For almost 2 min it was nearly the only auroral form to be seen (Fig. 10). It travelled rapidly towards the east with an increasing velocity up to 3 km s^{-1} until at 2121:43 its motion was suddenly stopped. Eight seconds later the structure had become partly wound up anticlockwise into a somewhat rayed spiral. It then dissolved rapidly, and developed into a rather intense north-south-aligned linear form above the Kola peninsula. This was accompanied by the appearance

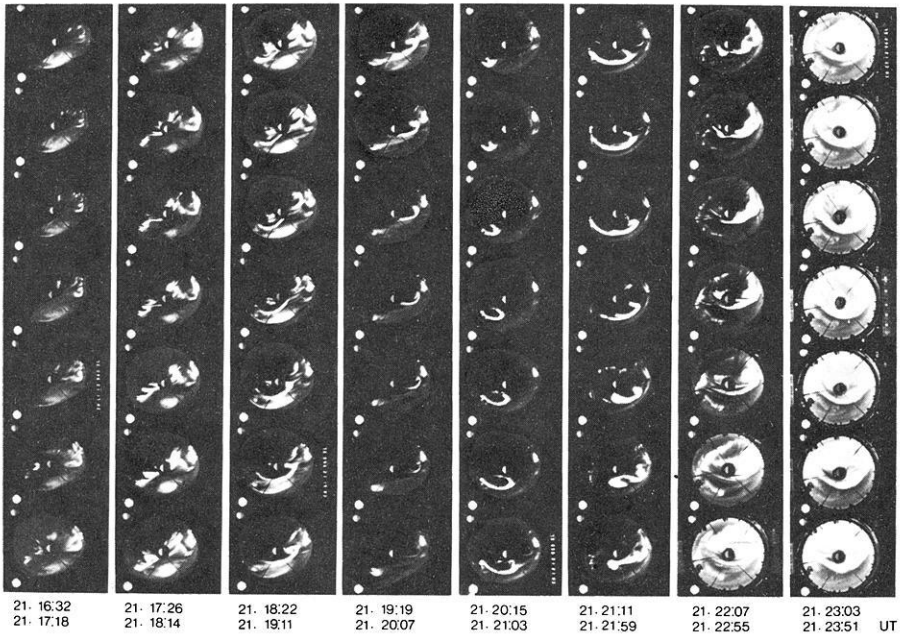

Fig. 10. All-sky camera records from the station Ivalo for a time interval a few minutes before and around auroral breakup. Below each row time of uppermost and lowest frame is indicated. Geographic north is upwards, east is to the right

of rayed auroral forms in the northwest of the region under observation. At 2122:31 UT all the formerly existing forms intensified extremely, and at 2122:51 UT nearly the whole sky of the northern part of the region was covered with bright aurorae (Fig. 10). We may conclude that the auroral breakup occurred at about 2122:30 UT above northern Scandinavia.

During the breakup, the equivalent current system over Scandinavia changed drastically into a broad south-westward directed flow (Fig. 5, cf. current system at 2125 UT). The magnetic onset at our northernmost stations was extremely sharp, especially in the D- or B-components (cf. Fig. 3), and occurred between 2122:00 and 2122:10 UT.

This magnetic onset was accompanied by an intense Pi B event observed especially at Kevo and Sodankylä (and possibly preceded by another weaker event one minute earlier) (cf. Fig. 7), and by a clear Pi 2 event at middle European magnetic observatories (e.g., Wingst and Göttingen). As may be seen from Figure 2 the onset occurred at the beginning of worldwide substorm activity. The magnetograms from observatories to the east (Dixon, Cape Cheluskin) possibly indicate an onset 1–2 min earlier.

Note that at our stations in and near Scandinavia the magnetic behaviour is quite different (Fig. 3). Whereas at the western stations (profile between MIK and PIT) B is especially affected by the onset, the eastern stations show the main changes in A and Z. If we neglect the observations within the Scandinavian region the observations to the east on the nightside of the northern

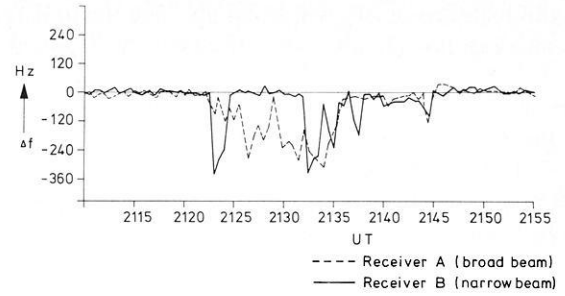

Fig. 11. Mean Doppler shift as a function of time as recorded by auroral radio wave backscatter receivers at Lycksele (cf. Fig. 1 for corresponding backscatter regions, denoted there by letters BL)

hemisphere probably indicate the switching on of an additional westward auroral electrojet of large longitudinal extent with corresponding field-aligned currents at the ends. The central meridian of this Birkeland type current system (cf. Kisabeth 1972) probably was located at about 03 MLT according to the magnetograms from the southern part of the Soviet Union (partly shown in Fig. 2), i.e., eastward from Scandinavia (00 MLT).

Simultaneously with the auroral breakup and the magnetic onset the Finnish riometers indicate a sharp onset of >40 keV electron precipitation above Kevo and Ivalo (Fig. 9). It is also observable at Tromsö and, though being a little more gradual and less intense, at Kiruna. At Kevo the maximum absorption difference amounts to 3.3 dB. Stations to the north and west of Scandinavia recorded only smooth delayed increases in absorption after the breakup. Eastward of Finland the strong absorption started before the observed breakup, showing a typical morningside behaviour with slow increase in absorption and delayed maxima (3 dB at Dixon Island at 2130 UT). On the dayside in Alaska small absorption started around 2040 UT, reaching 1 dB at around 2100 UT; after that the absorption decreased gradually.

As regards the radio wave backscatter receiver stations, Nurmijärvi (corresponding to the backscatter region BN in Fig. 1) received no signal. Sodankylä (region PS) showed a small precursor at 2118 UT followed by a fade, and then a sharp onset of a very strong signal at 2121:30 UT. At Lycksele (backscatter region BL) receivers A and B both recorded strong signals and negative Doppler shift from 2122 UT on, but with important differences (Fig. 11). Whereas receiver A (broad beam) showed a very gradual increase in signal amplitude and negative Doppler shift, both amplitude and shift at receiver B (narrow beam) appeared in a steplike fashion half a minute later and persisted for only 2 min. This means that backscattering was not uniformly distributed over the whole backscatter region belonging to receiver A, but was concentrated mostly to the part near Tromsö (crosshatched part of region BL in Fig. 1). The difference of the onset times indicates a westward propagation of the backscattering irregularities after the breakup over Kevo.

4. Discussion and Conclusions

Our further discussion will be concentrated upon the observed relationship between the early electrojet development and the accompanying auroral activity including spiral formation, and upon the phenomena at the time and around

the location of auroral breakup. The auroral fading which we observed before breakup has already been discussed by Pellinen and Heikkila (1978).

Pre-Onset Westward Electrojet System

Often it has been assumed that the northern and southern borders of an auroral electrojet are given by the locations of the extrema of Z as observed on the ground along a meridian chain of magnetometers (e.g., Wallis et al., 1976). This is correct for a broad electrojet. On the other hand, if the width becomes small as compared to the height h of the current, the north-south distance 2s between the minimum and maximum of Z approaches the value 2h. For a homogeneous sheet current of finite width 2w the relation $s=(w^2+h^2)^{1/2}$ holds, and the height-integrated current intensity J may be calculated from the values of the two Z extrema or from the H (or A) extremum value. Of course, it has to be assumed that internal contributions to the observed magnetic field at the ground are negligible. The smallness of such contributions has been verified for Scandinavia for slowly varying electrojets like the present one (U. Mersmann and K. Lange, priv. comm.). Also it is necessary that we are located far enough from the eastern ends of the electrojet. As was mentioned above, according to the small B variations before breakup this condition seems to be fulfilled in our case.

Accordingly, position (from the Z=O locations), width 2w (assuming h= 100 km), and height-integrated current intensity J have been calculated from the Z and A latitude profiles that are shown in Figure 6. The results are represented in Figure 12 (parts a and b), together with the location of the observed arcs above our meridian chain of magnetometers. With one exception, the southernmost arc is located within the northern half of the electrojet all the time. As was mentioned already, the electrojet and the southernmost arc travel southward in parallel. Note especially the slowing down or even interruption of the southward motion of both electrojet and auroral arc which occurs at 2050 UT. A common southward velocity averaged over 15 min has been calculated for the electrojet and for the southernmost arc. The results are also shown in Fig. 12b, both as a velocity and as an equivalent westward electric field E_{eq} (defined as the field which would give the observed motion if it were due to an $\mathbf{E}\times\mathbf{B}$ drift).

At the beginning of our interval E_{eq} is constant whereas J increases steadily. It seems as if the minimum of J occurring at 2050 UT is related to the deep decrease of E_{eq} at this time. Indeed, the quotient J/E_{eq} here called Σ_{eff} (effective height-integrated conductivity) and delineated in Figure 12c is steadily increasing all the time up to 2055 UT.

The question may be asked why the first hook-like distortions of the auroral arc (Sect. 3 and Fig. 4) appeared at 2055 UT. Apparently, no one of the three electrojet parameters 2w, J, and E_{eq} exhibits any peculiarity at this time, whereas Σ_{eff} shows a sharp maximum possibly indicating an extremum of height-integrated conductivities and therefore of particle precipitation over the 200 km wide latitudinal electrojet range.

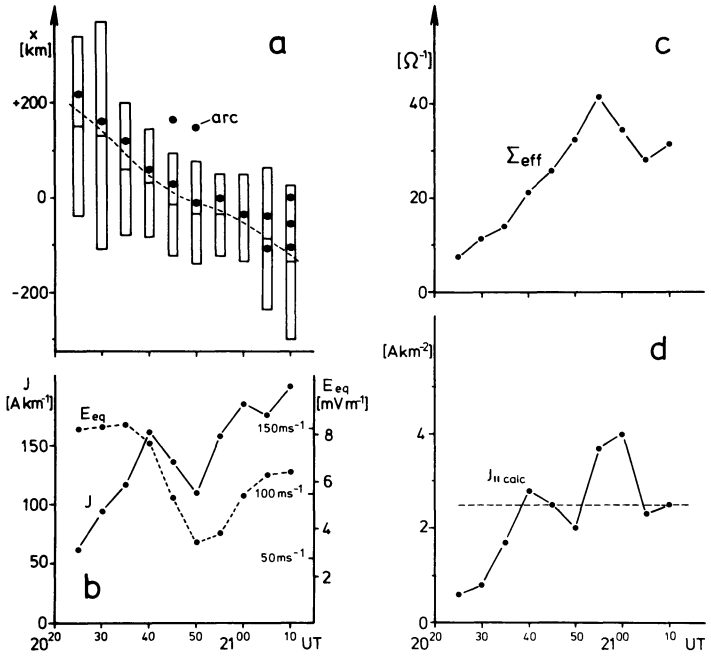

Fig. 12a–d. Different parameters derived from observations of pre-onset electrojet (Fig. 6) and auroral arcs, as functions of time. **a** Width 2w and position (vertical bars) of equivalent homogeneous ionospheric sheet current, and position of arcs (dots). **b** Intensity J of sheet current and smoothed southward velocity (scale to the right) of electrojet and southernmost arc, expressed as an equivalent westward electric field Σ_{eq} (according to $\mathbf{v}=\mathbf{E}\times\mathbf{B}/B^2$). **c** $\Sigma_{eff}=J/E_{eq}$. **d** $j_{\parallel calc}=\Sigma_H\Sigma_P^{-1}\,J\;w^{-1}$ as an order-of-magnitude estimate of the field-aligned current intensity, under the assumption of model B1 from Figure 13. The broken line indicates Hallinan's (1976) critical value, for comparison

On the other hand, it seems to be probable that the observed hook-like distortions constitute the beginning of spiral formation which requires a certain critical intensity of upward field-aligned currents, according to the theory developed by Hallinan (1976). Therefore, it may be useful to try to estimate at least by an order of magnitude calculation the field-aligned current directions and intensities from the above derived electrojet parameters.

There are two basic mechanisms by which an electrojet at high latitudes may be generated (Boström, 1964, 1977): The first mechanism (Fig. 13, part A) regards the magnetosphere as a current or voltage generator. According to this model the field-aligned current within two vertical parallel sheets above the borders of the electrojet or the voltage between these two sheets are given. The two antiparallel field-aligned sheet currents are closed via Pedersen currents within the ionosphere. The corresponding Hall current constitutes the electrojet. For a westward electrojet (our case) the field-aligned currents above its northern border flow downward.

In the second mechanism (Fig. 13, parts B) that part of the magnetosphere which is connected to the central part of the electrojet (i.e., the part in the middle between its eastern and western ends) along the magnetic field lines

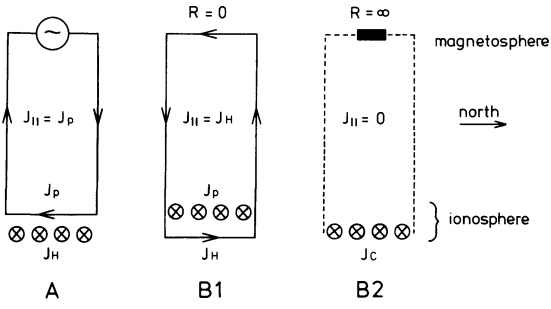

Fig. 13. Three mechanisms by which a westward polar electrojet (crossed circles) may be generated. In Model A the magnetosphere acts as a generator, the ionospheric electric field (southward) is limited to the electrojet region. Models B imply a large-scale westward ionospheric electric field. J_P Pedersen current, J_H Hall current, J_C Cowling current, J_{II} field-aligned current

acts as a load. The source of the electrojet is a large-scale ionospheric electric field $\mathbf{E}_0$ – generally generated by large-scale magnetospheric processes – which meets a local channel of higher conductivity. Because the current has to be source-free, eventually electric space charges will accumulate at the boundaries of the well conducting channel. Depending on the circumstances the electrojet may consist mainly of Hall or of Pedersen currents. Of critical importance are the horizontal direction of $\mathbf{E}_0$, the resistance R of the magnetospheric load between the two current sheets, and the contrast of conductivities outside and inside the channel.

The observed southward motion of the electrojet and of the accompanying arc suggests that a large-scale ionospheric electric field $\mathbf{E}_0$ with a westward component equal to E_{eq} (Fig. 12b; see Kelley et al. (1971) for justification of this latter assumption) was present, indeed. According to Mozer (1971), a westward electric field of the order of 10 mVm^{-1} typically appears during the hour preceding a substorm onset around magnetic midnight. For that reason, we consider first the consequences of applying the second mechanism to our case.

According to the magnetic A-component latitude profiles shown in Figure 6 the electrojet clearly stands out above the background to the north and south where the ionospheric currents generally seem to be rather small. We assume therefore, that the conductivities outside the electrojet region may be neglected. This excludes the possibility that the north-south component of $\mathbf{E}_0$, if present, was of any importance for electrojet generation because due to the non-divergence of currents the corresponding Pedersen currents – and therefore the Hall currents also – would have been negligible within the conductivity channel.

The westward component of $\mathbf{E}_0$ renders an upward directed field-aligned sheet current of intensity $J_\parallel = (\Sigma_H/\Sigma_p)J$ above the northern border of the electrojet if the resistance of the mentioned magnetospheric load is assumed to be negligible (case B1 in Fig. 13). Here, Σ_H and Σ_P denote the height-integrated Hall and Pedersen conductivity, respectively, and J means the derived electrojet current density as shown in Figure 12b. In this case, the electrojet is a pure Pedersen current, and Σ_{eff} (Fig. 12c) has to be interpreted as Σ_P. If, on the other hand, the magnetospheric resistance is assumed to be infinitely large, the field-aligned currents are suppressed completely, and the electrjet is a Cowling current with $\Sigma_{eff} = \Sigma_P + \Sigma_H^2 \Sigma_P^{-1}$ (case B2 in Fig. 13).

In reality, $J_\parallel$ will be distributed over a horizontal north-south range of the order of w (see Fig. 12a). This gives a field-aligned current density of the order of $j_{\parallel calc} = J_\parallel / w$. Under the assumption that model B1 (Fig. 13) holds, this quantity is equal to the values shown in Figure 12d if a value of 2 is inserted for the ratio Σ_H/Σ_P as indicated by results given by Evans et al. (1977), De La Beaujardiere et al. (1977), and Horwitz et al. (1978). It seems remarkable that the above-mentioned first hook-like auroral distortions appear at the time (2055–2100 UT, see Fig. 4) when our calculated values of field-aligned current density (Fig. 12d) for the first time substantially surpass the critical value 2.5 A km^{-2} given by Hallinan (1976). On the other hand, it seems to be unacceptable to interpret the Σ_{eff}-values as shown in Figure 12c correspondingly as height-integrated Pedersen conductivities, because outside auroral arcs Σ_P generally is of the order of only 10 Ω^{-1} (Horwitz et al., 1978). We conclude therefore, that it seems to be possible to interpret our electrojet observations within the framework of model B (Fig. 13), but only if at least some part of the field-aligned current is suppressed by finite magnetospheric resistance.

Rocket experiments (see, for example, Anderson and Vondrak, 1975; Casserly, 1977) and theoretical considerations (Sato, 1978; for example) have shown that an auroral arc is connected to a quite local (north-south range a few tens of kilometers) system of field-aligned currents and one or two electrojets. The upward directed field-aligned current flows above the arc, and it is the intensity of this current which seems to be critical for the development of auroral spirals (Hallinan, 1976). As Sato (1978) has pointed out the local arc current system may develop under quite different circumstances (different directions of $\mathbf{E}_0$, for example). We conclude therefore, that in our case not only a mixture between the models B1 and B2 (Fig. 13) is capable of explaining the observations of electrojet growth and spiral formation. Model A or a pure model B2 may be considered as well.

Model A yields downward field-aligned currents above the northern half of the electrojet (Fig. 13), i.e., within the region where upward current is necessary for explanation of the observed spiral formation. As may be seen from Figure 13, the order of magnitude of this downward current would amount to (Σ_P/Σ_H)J w^{-1} and would therefore be smaller than the values shown in Figure 12d by a factor of 4 (if again $\Sigma_H/\Sigma_P = 2$ is assumed). This background of downward currents of intensities well below Hallinan's (1976) critical value all the time would probably not impede spiral growth if the local mechanism of arc formation proposed by Sato (1978) is going on which seems to render upward currents above the arc of the order of 10 A km^{-2} in cases like the present one.

Auroral Breakup Current System

The second item which we intend to discuss more thoroughly is the electric current system around the time of the observed auroral breakup and of the strong absorption event (2122 UT, cf. Figs. 4, 9 and 10). The Scandinavian magnetograms (Fig. 3) suggest that an additional current system had been switched

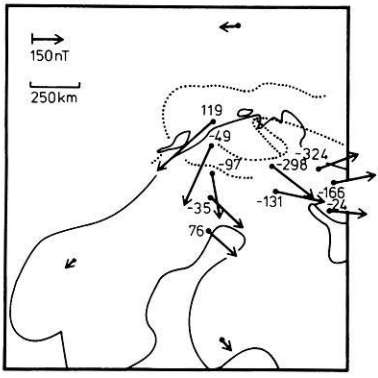

Fig. 14. Main auroral structures (dotted) immediately after breakup at 2125 UT, and differential equivalent current vectors calculated for the time difference 2122 and 2125 UT (cf. Fig. 8). Numbers indicate corresponding Z differences (in nT)

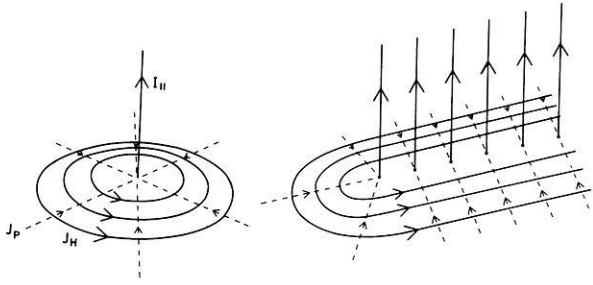

Fig. 15. Schematic view of a current system (right) which may be able to explain the pattern of equivalent current vectors shown within Figure 13. It is composed of elementary systems (Fukushima, 1971) as shown to the left. J_P and J_H denote the Pedersen and Hall currents, respectively

on very abruptly, at this time. Assuming that the preexisting current system (Fig. 5, system at 2122 UT) had remained constant we get the additional (differential) equivalent current vectors shown in Figure 14. These vectors seem to encircle the region where the auroral breakup and the strong absorption event have been observed, i.e., the region of most intense particle precipitation. The differential equivalent current vectors suggest that this was a region of intense upward field-aligned current according to the already mentioned model of Fukushima (1971), shown schematically in Figure 15 (left part). On the other hand the Z variations from our easternmost stations (cf. Fig. 3, and Z values given in Fig. 14) indicate that the differential equivalent current system may be rather elongated towards the east, and that accordingly the field-aligned current would be more similar to a current ribbon (Fig. 15, right part) with its western boundary above Scandinavia, than to a line current.

Figure 14 in connection with Figure 15 indicates that during breakup strong southward Hall currents, i.e., strong northward E-region electron drifts are generated only in the longitudinally confined region near Tromsö (magnetic stations MIK and ROS, cf. Fig. 1). Qualitatively at least this is in accordance with the negative Doppler shifts (Fig. 11) observed at Lycksele from the backscatter region denoted by letters BL in Figure 1. Furthermore, the amazing

differences (see above) between the large amplitude and Doppler shift (Fig. 11) recorded by the narrow beam receiver A (cf. small crosshatched backscatter region near Tromsö in Fig. 1) and the much smaller shift recorded by the broad beam receiver B between 2122 and 2124 UT may be due to this longitudinal confinement of strong electron drifts. If we assume that the electron drift vector was not too far from being parallel to the line of sight of the backscatter transmitter – receiver system, we may deduce an eastward electric field with a strength of 15 mV m^{-1} from the – 250 Hz Doppler shift observed by receiver B, for the region near our magnetic stations ROS and MIK. On the other hand, the 300 nT change recorded in the D component at these two stations between 2122 and 2124 UT indicates a height-integrated southward Hall current density of 0.5 Am^{-1} (calculated from the formula for an infinite current sheet). Because of the lateral inhomogeneity of the current system (which also justifies the neglect of internal field contributions) this will be an underestimate. The ratio of the two quantities gives a height-integrated Hall conductivity of about 50 Ω^{-1} for this region which seems to be quite realistic (Brekke et al., 1974; De La Beaujardiere et al., 1977).

Our magnetic observations during the auroral breakup show some similarity to the observations reported by Kisabeth and Rostoker (1973) for the case of a westward travelling surge passing their meridian chain of stations. This regards especially the large disturbances in the D component. On the other hand, our optical observations indicate essentially a local auroral breakup, and not passing of a preexisting auroral form. Furthermore, the traces on our magnetic records show a sharply defined (within less than 10 s) inflection, instead of a more gradual increase which has to be expected if a stationary overhead current system is approaching the station with constant and reasonable velocity.

Kisabeth and Rostoker (1973) have interpreted their observations by a north – south shear in the ionospheric part of a Birkeland current loop (Fig. 9 within their paper). Probably this would be an alternative interpretation in our case. The main difference seems to be that their model does not include local field-aligned currents. On the other hand, in another paper Rostoker (1974) has envisaged a single field-aligned current jumping to a new position during the substorm expansion phase, in the midnight region. This model comes nearer to our interpretation.

5. Summary

Our observations made shortly (1–0 h) before magnetic midnight between the time of the southward turning of the interplanetary magnetic field (2016 UT) and substorm onset (2122 UT) may be summarized in the following way:

1. A westward electrojet with generally increasing intensity appeared over northern Scandinavia. It may be modelled by a homogeneous sheet current of finite width. The corresponding sheet current density reached values near 200 A km^{-1} well before onset, whereas the width varied in a nonmonotonous way between 200 and 400 km.

2. An auroral arc, intermittently accompanied by parallel arcs to the north, was situated above the northern half of the electrojet.

3. Both electrojet and arc moved southward in parallel, with an average (2025–2110 UT) speed of 120 ms^{-1}. Around 2050 UT both electrojet and arc nearly discontinued their motion, intermittently.

4. Our riometers indicated weak ionospheric absorption above the same region at this time. The absorption region also moved towards south, with an estimated speed of 100–200 ms^{-1}.

5. From 2055 UT on, the arc was intermittently distorted with increasing intensity. The first distortions were shaped in a hook-like fashion, later on a mature spiral developed.

6. The first distortions appeared at a time when the field-aligned current intensity, estimated from the derived electrojet parameters by an order-of-magnitude calculation, reached values of the order of 1 A km^{-2}.

7. Nearby short period pulsation magnetometers indicated Pi B activity whenever the auroral arc was distorted.

8. During the few minutes of spiral growth and at the same location, an additional pattern of radially directed magnetic disturbance vectors at the ground appeared. This observation seems to indicate rather directly that the spiral enclosed a local region of upward directed field-aligned current.

9. At the time (2116 UT) of the last auroral intensification and distortion before the magnetic onset and the auroral breakup, in addition to the mentioned Pi B activity a first Pi 2 event was recorded in middle Europe, and weak auroral backscattering of radio waves occurred above northern Scandinavia.

As regards the southward drift of the auroral arc, the electrojet, and the absorption region, our observations seem to supplement results published by Pytte et al. (1976).

We think that it has to remain an open question whether our observations support the concept of the growth phase (McPherron, 1970). Perhaps the substorm under discussion was not isolated well enough. However, we must emphasize that nearly all the different ground-signatures which are thought to be evidence for a growth phase (McPherron, 1970; McPherron et al., 1973; Kokubun and Iijima, 1975; Vorobjev et al., 1976; Mozer, 1971; Hargreaves et al., 1975) have been observed by us and have been shown to be closely related.

About our results regarding the auroral breakup, which was observed exactly at magnetic midnight, the following may be stated:

1. The magnetic observations are interpreted by us by a model in which at the time and at the location of the breakup a current system is added to the preexisting electrojet which implies strong upward directed field-aligned current flow above the breakup region and a corresponding ionospheric Hall current circulation around it.

2. This interpretation seems to be supported by the fact that at the time of auroral breakup strong radio wave auroral backscatter signals with a large negative Doppler shift of frequency were received only from a small region, quite confined in longitude, immediately to the west of the breakup region, which was also a region of strong ionospheric absorption as indicated by the riometer observations. Furthermore, the value of the observed Doppler shift

is in accordance with the observed magnitude of the magnetic east-west disturbance at ground, if a reasonable value of the height-integrated Hall conductivity is assumed.

Acknowledgements. Our magnetic observations have been performed in cooperation with the Department of Plasma Physics of the Royal Institute of Technology at Stockholm, with the Kiruna Geophysical Institute, and with the Auroral Observatory at Tromsö. There, we got much help and scientific advice especially from Dr. R. Boström, Dr. G. Gustafsson, and Mr. St. Berger. For providing additional magnetic data, our thanks are due to Mr. H. Maurer from the Technical University of Braunschweig, Dr. G.A. Loginov from the Polar Geophysical Institute at Apatity, Mr. St. Berger from the Auroral Observatory at Tromsö, Dr. C. Sucksdorff from the Finnish Meteorological Institute, and to the World Data Center C1 at Copenhagen. Similarly, we are obliged to Dr. G. Gustafsson from the Kiruna Geophysical Institute for placing all-sky-camera records at our disposal. We wish to thank Dr. J. Vette from the Satellite Situation Center (SSC) at Goddard Space Flight Center, Greenbelt, Maryland, for providing data on the interplanetary magnetic field, and Dr. H. Voelker from the University of Göttingen who kindly sent us information on Pi 2 activity. We are also indebted to Dr. J. Kisabeth, Edmonton, for critical and very helpful comments during preparation of this paper, and to Dr. A. Jones, Münster, for critically reading the text.

The University of Münster part of this work has been supported financially by the Deutsche Forschungsgemeinschaft. One of us (W.J.H.) acknowledges support from the National Science Foundation.

References

Akasofu, S.-I.: Polar and magnetospheric substorms, Dordrecht: D. Reidel Publ. Comp. 1968

Akasofu, S.-I.: Physics of magnetospheric substorms. Dordrecht-Boston: D. Reidel Publ. Comp. 1977

Anderson, H.R., Vondrak, R.R.: Observations of Birkeland currents at auroral latitudes. Rev. Geophys. Space Phys. **13**, 243–262, 1975

Boström, R.: A model of the auroral electrojets, J. Geophys. Res. **69**, 4983–4999, 1964

Boström, R.: Current systems in the magnetosphere and ionosphere. In: Radar probing of the auroral plasma, A. Brekke, ed.: Proc. EISCAT Summer School, Tromsö, Norway June 5–13, 1975, Universitetsforlaget, Tromsö-Oslo-Bergen, 1977

Boyd, J.S., Belon, A.E., Romick, G.J.: Latitude and time variations in precipitated electron energy inferred from measurements of auroral heights. J. Geophys. Res. **76**, 7694–7700, 1971

Brekke, A., Doupnik, J.R., Banks, P.M.: Incoherent scatter measurements of *E*-region conductivities and currents in the auroral zone. J. Geophys. Res. **79**, 3773–3790, 1974

Casserly, R.T., Jr.: Observation of a structured auroral field-aligned current system. J. Geophys. Res. **82**, 155–163, 1977

Davis, T.N., Hallinan, T.J.: Auroral spirals, 1. Observations. J. Geophys. Res. **81**, 3953–3958, 1976

De La Beaujardiere, O., Vondrak, R., Baron, M.: Radar observations of electric fields and currents associated with auroral arcs. J. Geophys. Res. **82**, 5051–5062, 1977

Egeland, A.: Formation and movements of ionospheric irregularities in the auroral *E*-region. In: Radio systems and the ionosphere, AGARD Conference Proc. No. 173, W.T. Blackband, ed.: pp. 32-1–32-15, Adv. Group for Aerospace Res. and Development, Neuilly Sur Seine, 1976

Evans, D.S., Maynard, N.C., Trøim, J., Jacobsen, T., Egeland, A.: Auroral vector electric field and particle comparisons, 2. Electrodynamics of an arc. J. Geophys. Res. **82**, 2235–2249, 1977

Fukushima, N.: Electric current systems for polar substorms and their magnetic effect below and above the ionosphere. Radio Sci. **6**, 269–275, 1971

Gough, D.I., Reitzel, J.S.: A portable three-component magnetic variometer. J. Geomag. Geoelectr. **19**, 203–215, 1967

Gustafsson, G.: A revised corrected geomagnetic coordinate system. Ark. Geofys. **5**, 595–617, 1970

Hallinan, T.J.: Auroral spirals, 2. Theory. J. Geophys. Res. **81**, 3959–3965, 1976

Hargreaves, J.K., Chivers, H.J.A., Axford, W.I.: The development of the substorm in auroral radio absorption. Planet. Space Sci. **23**, 905–911, 1975

Heacock, R.R.: Two subtypes of type Pi micropulsations. J. Geophys. Res. **72**, 3905–3917, 1967

Horwitz, J.L., Doupnik, J.R., Banks, P.M.: Chatanika radar observations of the latitudinal distributions of auroral zone electric fields, conductivities, and currents. J. Geophys. Res. **83**, 1463–1481, 1978

Hyppönen, M., Pellinen, R., Sucksdorff, C., Torniainen, R.: Digital all-sky camera, Techn. Rept. No. 9, Finnish Meteorol. Inst., 1974

Kelley, M.C., Starr, J.A., Mozer, F.S.: Relationship between magnetospheric electric fields and the motion of auroral forms. J. Geophys. Res. **76**, 5269–5277, 1971

Kisabeth, J.L.: The dynamical development of the polar electrojets, PhD thesis, University of Alberta, Edmonton, 1972

Kisabeth, J.L., Rostoker, G.: Current flow in auroral loops and surges inferred from ground-based magnetic observations. J. Geophys. Res. **78**, 5573–5584, 1973

Kisabeth, J.L., Rostoker, G.: Modelling of three-dimensional current systems associated with magnetospheric substorms. Geophys. J. Roy. Astron. Soc. **49**, 655–683, 1977

Kokubun, S., Iijima, T.: Time-sequence of polar magnetic substorms. Planet. Space Sci. **23**, 1483–1494, 1975

Küppers, F., Untiedt, J., Baumjohann, W., Lange, K.: A two-dimensional magnetometer array for ground-based observation of auroral zone electric currents during the IMS. J. Geophys. **45**, in press, 1979

Lassen, K., Sharber, J.R., Winningham, J.D.: The development of auroral and geomagnetic substorm activity after a southward turning of the interplanetary magnetic field following several hours of magnetic calm. J. Geophys. Res. **82**, 5031–5050, 1977

McPherron, R.L.: Growth phase of magnetospheric substorms. J. Geophys. Res. **75**, 5592–5599, 1970

McPherron, R.L., Russell, C.T., Aubry, M.P.: Satellite studies of magnetospheric substorms on August 15, 1968, 9. Phenomenological model for substorms. J. Geophys. Res. **78**, 3131–3149, 1973

Meng, C.-I., Akasofu, S.-I.: A study of polar magnetic substorms, 2. Three-dimensional current system. J. Geophys. Res. **74**, 4035–4053, 1969

Mozer, F.S.: Origin and effects of electric fields during isolated magnetospheric substorms. J. Geophys. Res. **76**, 7595–7608, 1971

Pellinen, R.J., Heikkila, W.J.: Observations of auroral fading before breakup (accepted for publication) J. Geophys. Res., 1978

Pytte, T., Trefall, H.: Auroral-zone electron precipitation events observed before and at the onset of negative magnetic bays. J. Atmos. Terr. Phys. **34**, 315–337, 1972

Pytte, T., Trefall, H., Kremser, G., Jalonen, L., Riedler, W.: On the morphology of energetic ($\geqq$30 keV) electron precipitation during the growth phase of magnetospheric substorms. J. Atmos. Terr. Phys. **38**, 739–755, 1976

Rostoker, G.: Polar magnetic substorms. Rev. Geophys. Space Phys. **10**, 157–211, 1972

Rostoker, G.: Current flow in the magnetosphere during magnetospheric substorms. J. Geophys. Res. **79**, 1994–1998, 1974

Russell, C.T.: Geophysical coordinate transformations. Cosmic Electrodyn. **2**, 184–196, 1971

Russell, C.T., McPherron, R.L.: The magnetotail and substorms. Space Sci. Rev. **15**, 205–266, 1973

Sato, T.: A theory of quiet auroral arcs. J. Geophys. Res. **83**, 1042–1048, 1978

Snyder, A.L., Akasofu, S.-I.: Observations of the auroral oval by the Alaskan meridian chain of stations. J. Geophys. Res. **77**, 3419–3430, 1972

Troshichev, O.A., Kuznetsov, B.M., Pudovkin, M.I.: The current systems of the magnetic substorm growth and explosive phases. Planet. Space Sci. **22**, 1403–1412, 1974

Vorobjev, V.G., Gustafsson, G., Starkov, G.V., Feldstein, Y.I., Shevnina, N.F.: Dynamics of day and night aurora during substorms. Planet. Space Sci. **23**, 269–278, 1975

Vorobjev, V.G., Starkov, G.V., Feldstein, Y.I.: The auroral oval during the substorm development. Planet. Space Sci. **24**, 955–965, 1976

Wallis, D.D., Anger, C.D., Rostoker, G.: The spatial relationship of auroral electrojets and visible aurora in the evening sector. J. Geophys. Res. **81**, 2857–2869, 1976

Wescott, E.M., Stenbaek-Nielsen, H.C., Davis, T.N., Murcray, W.B., Peek, H.M., Bottoms, P.J.: The L=6.6 Oosik barium plasma injection experiment and magnetic storm of March 7, 1972. J. Geophys. Res. **80**, 951–967, 1975

Whalen, J.A.: Auroral oval plotter and nomograph for determining corrected geomagnetic local time, latitude, and longitude for high latitudes in the northern hemisphere, Environmental Res. Papers, No. 327, Air Force Cambridge Res. Lab., Bedford, Mass., 1970

Received July 14, 1978 / Accepted September 14, 1978